




High frequency near-infrared up-conversion single-photon imaging based on the quantum compressed sensing

HUIDAN BAI,^{1,2} SHUXIAO WU,^{1,2} ZHIXING QIAO,³  JIANYONG HU,^{1,2,*} RUIYUN CHEN,^{1,2}  CHENGBING QIN,^{1,2}  GUOFENG ZHANG,^{1,2} LIANTUAN XIAO,^{1,2,4} AND SUOTANG JIA^{1,2}

¹State Key Laboratory of Quantum Optics and Quantum Optics Devices, Institute of Laser Spectroscopy, Shanxi University, Taiyuan 030006, China

²Collaborative Innovation Center of Extreme Optics, Shanxi University, Taiyuan 030006, China

³College of Medical Imaging, Shanxi Medical University, Taiyuan 030001, China

⁴xlt@sxu.edu.cn

*jyhu@sxu.edu.cn

Abstract: Infrared up-conversion single-photon imaging has potential applications in remote sensing, biological imaging, and night vision imaging. However, the used photon counting technology has the problem of long integration time and sensitivity to background photons, which limit its application in real-world scenarios. In this paper, a novel passive up-conversion single-photon imaging method is proposed, in which the high frequency scintillation information of a near infrared target is captured by using the quantum compressed sensing. Through the frequency domain characteristic imaging of the infrared target, the imaging signal-to-noise ratio is significantly improved with strong background noise. In the experiment, the target with flicker frequency on the order of GHz is measured, and the signal-to-background ratio of the imaging reaches up to 1:100. Our proposal greatly improved the robustness of near-infrared up-conversion single-photon imaging and will promote its practical application.

© 2023 Optica Publishing Group under the terms of the [Optica Open Access Publishing Agreement](#)

1. Introduction

Near-infrared (NIR) optical imaging has essential applications in meteorological monitoring, gas analysis, medical imaging, and other fields [1–3]. However, the existing commercially available NIR imaging products suffer from low detection sensitivity, slow response, and susceptible to background noise, which limits their applications in extreme environments [4]. In contrast, silicon single-photon detectors (SPD) have the characteristics of high detection efficiency, low dark count rate and small time jitter, and can realize extremely sensitive imaging at the single-photon level [5,6]. Therefore, to convert infrared photons to visible wavelength and imaging with the high performance visible light sensor is a feasible technical route to improve the infrared imaging performance [7,8].

Since 1968, Midwinter from Malvern Royal Radar Institute demonstrated up-conversion imaging using lithium niobate crystal [9], the development of this technology has been continuously concerned by researchers [10]. In recent years, researchers have developed parametric mode sorting and gated filtering technologies based on up-conversion imaging, which effectively improve the imaging practicability in strong background environment [11,12]. However, the current NIR up-conversion single-photon imaging still uses the traditional photon counting technology, which has long integration time and low imaging frame rate, and unable to respond to the high frequency flicker of the measured target. Compressed sensing can recover the sparse signals in the transform domain with the sampling rate much lower than the Nyquist sampling rate, which has the potential to realize real-time, broadband signal detection [13–15]. However,

the existing CS imaging technology mainly studies the data compression in the two-dimensional space domain to improve the imaging frame rate, but does not realize the compression sampling in the time domain directly, and the ability to capture high-frequency flicker is still limited by low imaging frame rate [16–18].

In this paper, a novel passive up-conversion single-photon imaging method based on the quantum compressed sensing (QCS) is proposed, in which the characteristic spectrum information of high frequency flicker target can be obtained directly. By converting the NIR photons of the target to visible band, a mature visible SPD is used for single-photon detection. Although both the background noise photon and the signal photon are detected by the SPD, since the background noise does not have spectrum characteristics and presents as white noise distribution in the frequency domain, the signal can be distinguished from the background by frequency domain transformation, thus significantly improving the imaging signal-to-noise ratio (SNR). In the experiment, a single-photon imaging setup based on the point-by-point scanning is built. And the high frequency flicker target is constructed by an intensity modulated laser projection. NIR photons were detected by a visible SPD after frequency up-conversion through an optical nonlinear crystal, and the arrival time of each photon was recorded using a time-interval analyzer. The frequency domain information of the target is obtained and imaged by the data recovery algorithm, and the noise immunity of the imaging system is verified. In the experiment, the characteristic spectrum of high frequency flicker target on the order of GHz is successfully captured, and based on this, the imaging under the condition of 1:100 signal background ratio is realized. The proposed high-frequency up-conversion single-photon imaging scheme has the characteristics of high sensitivity, high frequencies and noise immunity, which opens a new technical path for the application of near-infrared single-photon imaging in real scenes.

2. Theoretical model of the quantum compressed sensing imaging

The high frequency NIR up-conversion single-photon imaging based on the QCS proposed in this paper is a combination of compressed sensing quantization and up-conversion imaging technology to improve the NIR imaging performance from both theoretical and technical aspects.

According to the classical sampling theorem, the sampling rate is required to be more than twice the bandwidth of the measured signal in order to recover the measured signal correctly [19]. The ideal signal sampling can be expressed as:

$$f_{(kT)} = \sum_{k=1}^N f_{(t)} \delta(t - kT) \quad (1)$$

After the sampling, the original signal $f_{(t)}$ is converted to $f_{(kT)}$ with sampling rate $f_s = 1/T$, where $k = 1, 2, \dots, N$ represents the sequence samples, and N is the total number of samples. After the sampling and quantization, the Discrete Fourier Transform of the signal could be expressed as:

$$F_{(\omega)} = \sum_{k=1}^N f_{(kT)} e^{-j\omega kT} \quad (2)$$

Therefore, a high sampling rate is required for real-time measurement of broadband signals, which causes great pressure on the hardware, including signal detection, data storage, and processing. Especially in imaging, the capture of high frequency flicker requires a high imaging frame rate. The real target often has sparse frequency domain characteristics. Compressed sensing can recover the sparse signals in the transform domain with the sampling rate much lower than the Nyquist sampling rate, which has the potential to realize real-time, broadband and high-resolution spectrum sensing. The QCS is a quantization of the classical compressed sensing, which realizes compressed sampling of the measured signal through quantum state preparation,

evolution and detection. Specifically, in this paper, QCS is realized by using random collapse behavior of photon wave function detection, and the measurement process can be intuitively expressed as follows:

$$F(\Delta) = \sum_{\omega \in \Omega} a_{\omega} e^{-j2\pi\Delta t} \quad (3)$$

where, a_{ω} represents the weights of different frequency components, Δ represents the spectral resolution; Ω denotes the set of K frequency components $\Omega = \{0, \pm 1, \pm 2, \dots, \pm K/2\}$, denoted the measurement bandwidth by W , the compressed sensing collected signal could be expressed by $R = \log_2(C(W/\Delta, K))$ bit information, where $C(W/\Delta, K) = (W/\Delta)! / (K!(W/\Delta - K)!)$. Therefore, in principle, only R samples are needed to obtain the required information.

In the experiment, we set the measured target as a pattern with periodic flickering, so it presents as a single frequency component in the frequency domain, which meets the prerequisite for sparsity of transform domain required by CS. Suppose that the imaging integration time is T , and a pixel in the image detects N photons within the integration time, the arrival time $t = t_1, t_2, \dots, t_N$ ($0 \leq t \leq T$) of each photon was recorded by the time interval analyzer. Since photon detection is a completely random process, corresponding to the random measurement matrix of CS, it satisfies the incoherence requirement of CS. The spectrum of the target signal was obtained by executing the Discrete Fourier Transform algorithm on the discrete random time series of each pixel:

$$F(\omega) = \sum_{n=1}^N A e^{i\omega t_n} \quad (4)$$

where A represents the amplitude coefficient, t_n is the arrival time sequence of photons. Since the SPD used in our experiment does not have the capability of photon number resolution, we normalize it here, that is, $A = 1$. Please refer to Ref. 20 for more details on the algorithm. Next, we extract the spectral characteristic peaks of all imaging pixels to obtain the frequency domain imaging of the target, for more detail please refer to Refs. [20,21]. Of course, the photon counting imaging can also be performed based on the collected data.

3. Experimental setup

Figure 1 shows the experimental setup of high-frequency NIR up-conversion single-photon imaging based on the QCS, which includes two parts: the target and the imaging system. In the experiment, the target is a fan pattern, where the mounting bracket is the static part and the fan blade is the flashing part of the pattern. The 1550 nm continuous lasers (DFB-1550-10-PM-FA-M) was divided into two beams by a beam splitter, one for projecting a static mounting bracket and the other for projecting a flashing blade. The high frequency scintillation is generated by an intensity modulator with sine function. The fan pattern is projected on a white board to form a projection image of 2cm*2 cm.

As to the imaging system, a high-precision closed-loop scanning mirror (Optotune, MR-E-2) is used to scan the fan projection pattern point by point. The collected near-infrared photons were completely coincided with the 1064 nm pump laser (MIL-N-1064-5W) through a dichroic mirror, and the mixed beam was focused on barium metaborate (β -BaB₂O₄, BBO, 8 × 8 × 7 mm³, $\theta = 20.6^\circ$, $\Phi = 0^\circ$) to convert 1550 nm NIR photons into 629.33 nm visible band. Pump induced parametric fluorescence background noise was removed by spectral filtering. Finally, photons were coupled to a 105 μ m multimode fiber using a 10× objective lens and detected by a visible SPD. A 631 nm laser is used to simulated the noise photons, and input the SPD directly. Meanwhile, the time interval analyzer is used to record the arrival time of each photon, and the high-frequency information of each pixel is extracted and the image is restored according to Eq. (4). In this experiment, up-conversion detection is adopted instead of using the InGaAs SPD directly. This is because visible SPD has smaller time jitter, which enables it to capture

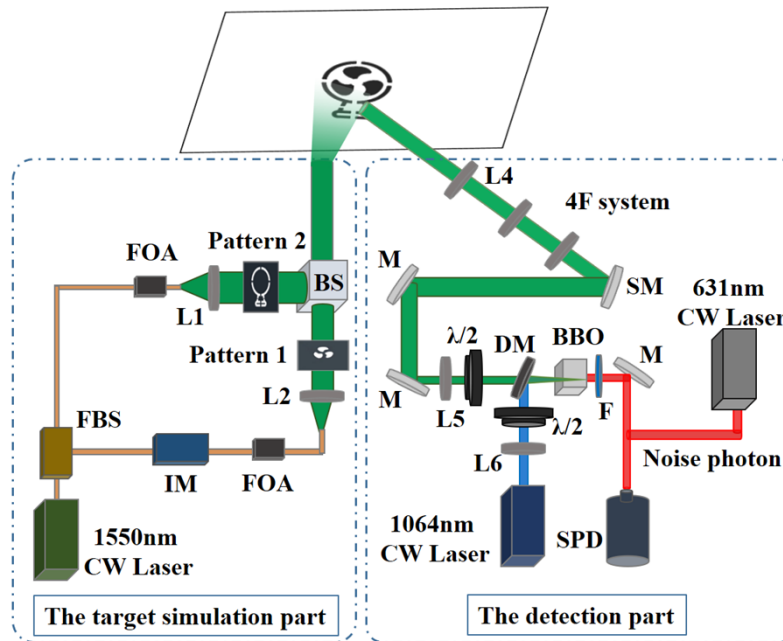


Fig. 1. Experimental setup of the passive up-conversion single-photon imaging. IM: intensity modulation; FOA: fiber optic amplifier; SM: scan mirror; DM: dichroic mirror; F: filter; BBO: β -BaB₂O₄, ($8 \times 8 \times 7$ mm³, $\theta=20.6^\circ$, $\Phi=0^\circ$); SPD: single-photon detector; M: mirror, L: lens.

higher frequency scintillation information. Meanwhile, mature visible SPD array provides the possibility for realizing efficient NIR imaging in the future.

4. Results and discussion

4.1. NIR up-conversion characterization

In the experiment, we first characterized the NIR up-conversion module, and the test results are shown in Fig. 2. After focusing, the 1550 nm signal light is coupled into the BBO crystal with 62% coupling efficiency, which is converted into 629.33 nm visible light under the action of 1064 nm pump laser, the spectral characterization is shown in Fig. 2(a). Frequency up-conversion efficiency is related to the optical power density of pump laser and signal light. When the pump power is much larger than the signal power, the up-conversion efficiency hardly varies with the signal power. However, with the increase of signal optical power the up-conversion efficiency decreases nonlinearly. In our experiment, when the signal optical power is 0.005 mW and the pump optical power is 4.16W, the up-conversion efficiency is 4.34%. However, the up-conversion efficiency drops sharply when the signal optical power reaches the mW level, as shown in Fig. 2(b), here, the pump optical power is fixedly set to 4.16W.

4.2. High frequency QCS single-photon imaging

The high frequency information extraction capability of the imaging system was characterized by an artificially constructed fan pattern. The pattern was scanned point by point with a high-precision scanning mirror, and the image pixel was set to 64×64 . In the experiment, images were measured when the integration time of a single pixel was 0.005s, 0.01s, 0.05s, 0.1s and 0.2s,

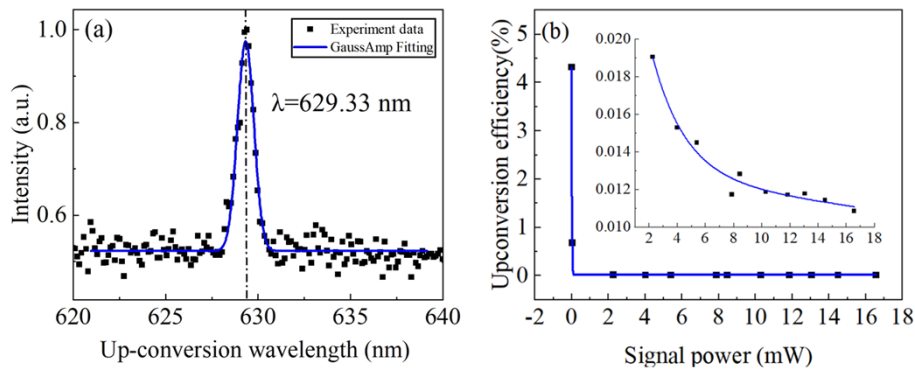


Fig. 2. Up-conversion performance characterization. (a) Up-conversion spectrum with a center wavelength of 629.33 nm. (b) Up-conversion efficiency vs signal optical power.

respectively, as shown in Fig. 3. We compared the traditional photon counting imaging with the QCS imaging proposed in this paper. Here, we set the flicker frequency of the fan blade to 1 MHz. Therefore, in the frequency domain, the pattern is presented as a single non-zero sequence located at 1 MHz, which satisfies the sparse condition required by compressed sensing. By recording the random arrival time of each pixel photon, the frequency domain information of the target is extracted by Eq. (4). Here, the random detection of photons corresponds to the measurement matrix in CS. Through comparison, it can be seen that with the increase of integration time, the image SNR increases significantly. However, photon counting imaging cannot distinguish the high frequency flicker region from the static region, while QCS imaging can obtain the frequency information of the image. When 1 MHz characteristic spectral lines are selected for imaging, the background noise of other frequency components, including static regions, is well suppressed to achieve high frequency imaging.

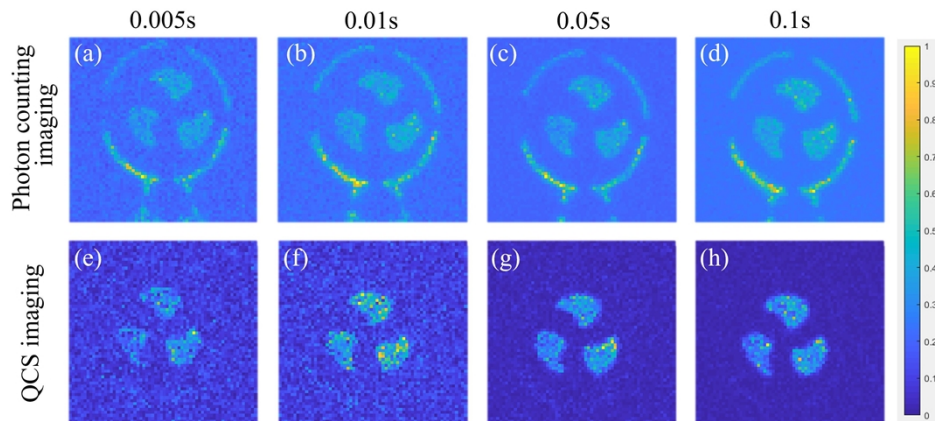


Fig. 3. Photon counting imaging and QCS imaging of high frequency flicker pattern. The first row is photon counting imaging, and the second row is the corresponding QCS imaging. The integration time of single pixel from left to right is 0.005s, 0.01s, 0.05s, and 0.1s, respectively.

In order to further clarify the relationship between the measurable bandwidth of the system, and the signal to noise ratio of the image, the frequency spectrum of single pixel of the image

was quantitatively analyzed. Here we define the imaging SNR as:

$$SNR = 10\log_{10}\left(\frac{\bar{\mu}_{signal}}{\sigma_{noise}}\right) \quad (7)$$

Figure 4 shows the variation of QCS imaging SNR as a function of target flicker frequency and measurement integration time. The target flicker frequency varies from 1kHz to 2 GHz, and the imaging SNR gradually decreases with the increase of the frequency, as shown in Fig. 4(a). This is because the measurement of high-frequency signals requires high-precision time measurement, and the measurement accuracy of photon arrival time in this experiment is limited by the time jitter of the SPD and the resolution of the time-interval analyzer, which is in the order of hundred picoseconds. Figure 4(b) shows the change of imaging SNR when the integration time varies from 0.1s to 1s. It can be seen from the figure that with the increase of integration time, the imaging SNR improves. On the one hand, this is because the background noise, such as the dark count of a SPD, is completely randomly distributed in the time domain, therefore, shows as white noise distribution in the frequency domain, refer to Ref. [20] for more details. The signal to be detected is sparse in frequency domain. With the increase of integration time, the amplitude of white noise in frequency domain shows a square relation with photon counting, while the amplitude of characteristic spectral line increases linearly with photon counting. On the other hand, there is quantum shot noise for single-photon detection. With the increase of photon count, the fluctuation caused by shot noise is gradually weakened, and the imaging SNR is also improved.

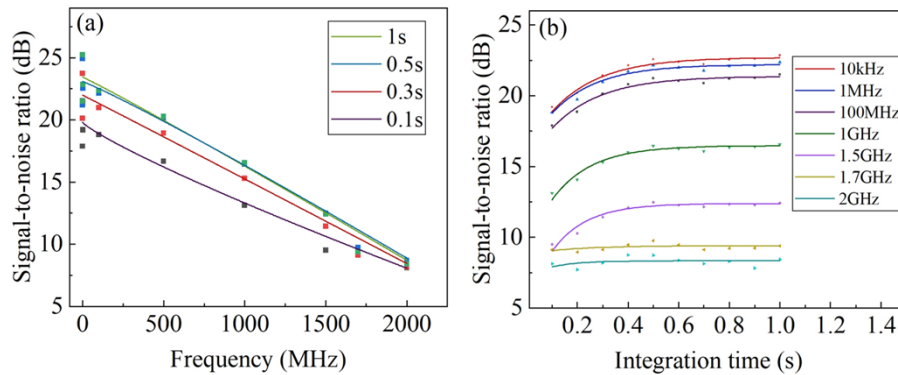


Fig. 4. The variation of QCS imaging SNR as a function of target signal frequency and measurement integration time. (a) Relationship between target signal frequency and imaging SNR. (b) Relationship between integration time and imaging SNR, where the mean photon count rate is set to 15kcps (count per second).

4.3. QCS single-photon imaging with high background

To investigate the noise immunity of the imaging system, on the basis of the high frequency QCS imaging, we designed an up-conversion single-photon imaging experiment with high background noise. Specifically, set the signal photon count to 15 kcps, the background is simulated by an additional light source. The background noise photon count is adjusted through a variable optical attenuator. In the experiment, the modulation frequency of fan-blade pattern was set as 1 MHz, and the signal-to-background ratio (SBR) varied from 1:1 to 1:100. The target patterns with different SBR were imaged, respectively, as shown in Fig. 5, the imaging pixel is 64×64 , and the integration time of each pixel was set as 0.5 s. We compared the traditional photon counting imaging and the QCS imaging, respectively. When the SBR is 1:20, the photon counting imaging

can no longer distinguish the signal from the background, while when the SBR is 1:100, the QCS imaging is still clear. The experimental results show that the QCS imaging proposed in this paper can extract the NIR high-frequency information in the extreme case of high background noise, which is two orders of magnitude higher than the target signal.

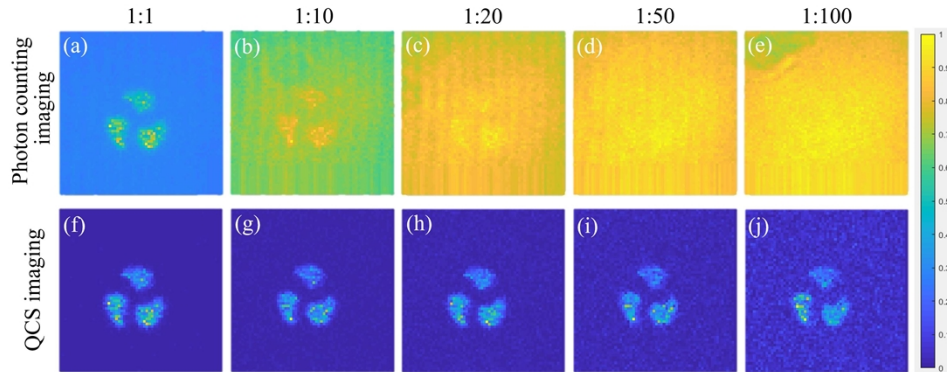


Fig. 5. Comparison of photon counting imaging and QCS imaging of fan-blade pattern with high background noise.

Through the analysis of single pixel data, we quantitatively studied the noise immunity of QCS imaging and compared it with the traditional photon counting imaging. As shown in Fig. 6, (a) and (b) are QCS imaging and photon counting imaging, respectively. With the increase of integration time, the imaging SNR is both improved. However, with high background noise, the SNR of photon counting imaging is lower than 0 dB, which means that the signal is completely submerged in the background noise and the imaging cannot be implemented. For QCS imaging, the SNR is improved by >10 dB compared with photon counting imaging, high frequency single-photon imaging can still be achieved in high background environment.

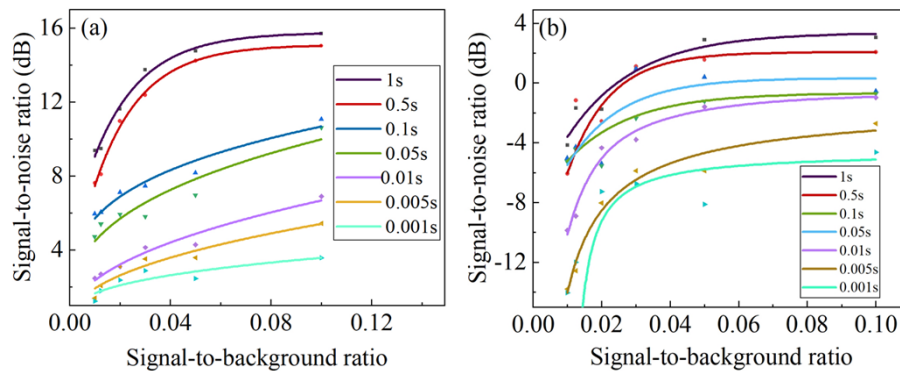


Fig. 6. Imaging SNR with high background noise. (a) Relationship between SNR and SBR of QCS imaging. (b) Relationship between SNR and SBR of photon counting imaging.

5. Summary

In this paper, a novel passive up-conversion single-photon imaging method based on the QCS is proposed. The spectrum features of high frequency flicker infrared target are extracted by the QCS algorithm, which improves the imaging bandwidth significantly. With QCS imaging of infrared target signal, the influence of background noise is effectively weakened, and the

imaging SNR of the system in the noisy environment is improved. In the experiment, we realized the target imaging with flicker frequency on the order of GHz, which is 9 orders of magnitude higher than the existing photon counting imaging. The imaging SBR reaches 1:100, which is two orders of magnitude higher than photon counting imaging. The proposal can not only be used for NIR imaging, but also for single-photon imaging of other wavelengths, which will significantly improve the measurable bandwidth and noise immunity of single-photon imaging, and open up a new technical path for the application of single-photon imaging in practical scenes.

Funding. 111 Project (D18001); Program for Changjiang Scholars and Innovative Research Team in University (IRT_17R70); National Natural Science Foundation of China (61875109, 62011530047, 62075120, 62075122, 62105193, 62127817, 91950109).

Disclosures. The authors declare no conflicts of interest.

Data availability. Data underlying the results presented in this paper are not publicly available at this time but may be obtained from the authors upon reasonable request.

References

1. W. P. Menzel, D. Tobin, and H. Revercomb, "Infrared Remote Sensing with Meteorological Satellites," *Adv. At., Mol., Opt. Phys.* **65**, 193–264 (2016).
2. H. Wang, X. Mu, J. Yang, Y. Liang, X. Zhang, and D. Ming, "Brain imaging with near-infrared fluorophores," *Coord. Chem. Rev.* **380**, 550–571 (2019).
3. G. Hong, A. Antaris, and H. Dai, "Near-infrared fluorophores for biomedical imaging," *Nat. Biomed. Eng.* **1**(1), 0010 (2017).
4. A. Singh and R. Pal, "Performance of InGaAs short wave infrared avalanche photodetector for low flux imaging," *Appl. Phys. A* **123**(11), 701 (2017).
5. C. Bruschini, H. Homulle, I. M. Antolovic, S. Burri, and E. Charbon, "Single-photon avalanche diode imagers in biophotonics: review and outlook," *Light: Sci. Appl.* **8**(1), 87 (2019).
6. S. Gundacker and A. Heering, "The silicon-photomultiplier: fundamentals and applications of a modern solid-state photon detector," *Phys. Med. Biol.* **65**(17), 17TR01 (2020).
7. S. Baldelli, "Sensing: Infrared image upconversion," *Nat. Photonics* **5**(2), 75–76 (2011).
8. K. Huang, X. Gu, H. Pan, E. Wu, and H. Zeng, "Two-dimensional infrared imaging by frequency upconversion at few-photon level," in *Quantum Electronics and Laser Science Conference* (2012) paper QF2G-1.
9. J. E. Midwinter, "Image conversion from 1.6 μm to the visible in lithium niobate," *IEEE J. Quantum Electron.* **4**(5), 319–320 (1968).
10. A. Barh, P. J. Rodrigo, L. Meng, C. Pedersen, and P. Tidemand-Lichtenberg, "Parametric upconversion imaging and its applications," *Adv. Opt. Photonics* **11**(4), 952–1019 (2019).
11. P. Rehai, Y. M. Sua, S. Y. Zhu, I. Dickson, B. Muthuswamy, J. Ramanathan, A. Shahverdi, and Y. P. Huang, "Noise-tolerant single photon sensitive three-dimensional imager," *Nat. Commun.* **11**(1), 921 (2020).
12. B. Wang, M. Y. Zheng, J. J. Han, X. Huang, X. P. Xie, F. H. Xu, and J. W. Pan, "Non-line-of-sight imaging with picosecond temporal resolution," *Phys. Rev. Lett.* **127**(5), 053602 (2021).
13. D. L. Donoho, "Compressed sensing," *IEEE Trans. Inf. Theory* **52**(4), 1289–1306 (2006).
14. Y. Tsaig and D. Donoho, "Extensions of compressed sensing," *Signal Processing* **86**(3), 549–571 (2006).
15. H. Hagihara, N. Namekata, K. Yokota, and S. Inoue, "Near infrared single-photon imaging based on compressive sensing with a sinusoidally gated InGaAs/InP single-photon avalanche diode," *Proc. SPIE* **11295**, 112950R (2020).
16. G. Howland, P. Dixon, and J. Howell, "Photon-counting compressive sensing laser radar for 3D imaging," *Appl. Opt.* **50**(31), 5917–5920 (2011).
17. X.-F. Liu, X.-R. Yao, C. Wang, X.-Y. Guo, and G.-J. Zhai, "Quantum limit of photon-counting imaging based on compressed sensing," *Opt. Express* **25**(4), 3286–3296 (2017).
18. L. Zhu, W. Zhang, D. Elnatan, and B. Huang, "Faster STORM using compressed sensing," *Nat. Methods* **9**(7), 721–723 (2012).
19. C. E. Shannon, "A mathematical theory of communication," *The Bell Syst. Tech. J.* **27**(3), 379–423 (1948).
20. J. Hu, Y. Liu, L. Liu, B. Yu, G. Zhang, L. Xiao, and S. Jia, "Quantum description and measurement for single photon modulation," *Photonics Res.* **3**(1), 24–27 (2015).
21. J. Hu, M. Jing, G. Zhang, C. Qin, L. Xiao, and S. Jia, "Performance of single-photons communication using the multi-channel frequency coding scheme," *Opt. Express* **26**(16), 20835–20847 (2018).